Applied Physics Letters

Actively tunable photonic crystal-based switch via plasmon-analog of index enhancement

Cite as: Appl. Phys. Lett. **119**, 211103 (2021); https://doi.org/10.1063/5.0071984
Submitted: 18 September 2021 • Accepted: 05 November 2021 • Published Online: 23 November 2021

Emre Yüce, Zafer Artvin, Ramazan Sahin, et al.

View Online
Export Citation
CrossMark

AIP Publishing

© 2021 Author(s).

Applied Physics Letters ARTICLE scitation.org/journal/apl

Actively tunable photonic crystal-based switch via plasmon-analog of index enhancement

Cite as: Appl. Phys. Lett. **119**, 211103 (2021); doi: 10.1063/5.0071984
Submitted: 18 September 2021 · Accepted: 5 November 2021 ·
Published Online: 23 November 2021

View Online Export Citation CrossMark

Emre Yüce,[1,2] Zafer Artvin,[3,4,5] Ramazan Sahin,[6] Alpan Bek,[1,2] and Mehmet Emre Tasgin[3,a)]

AFFILIATIONS

[1]Department of Physics, Middle East Technical University, 06800 Ankara, Turkey
[2]Center for Solar Energy Research and Applications (GÜNAM), Middle East Technical University, 06800 Ankara, Turkey
[3]Institute of Nuclear Sciences, Hacettepe University, 06800 Ankara, Turkey
[4]Department of Nanotechnology and Nanomedicine, Hacettepe University, Ankara, Turkey
[5]Central Laboratory, Middle East Technical University, 06800 Ankara, Turkey
[6]Faculty of Science, Department of Physics, Akdeniz University, 07058 Antalya, Turkey

[a)]Author to whom correspondence should be addressed: metasgin@hacettepe.edu.tr

ABSTRACT

We propose a miniaturized photonic switch, which utilizes (recently discovered) plasmon analog of index enhancement. An index is tuned via a control (auxiliary) pulse. The operation principle of the proposed device, composed of a few layers of nanorod dimers, is different than the conventional photonic switches. In the proposed device, a stop band is created at the desired frequency determined by the control pulse frequency. Calculated modulation depths are quite large, and response time is determined by the plasmon lifetime. The method we propose here is based on linear operation that requires low power and has very small foot-print that satisfies the major needs to be the choice of a switching scheme for integrated optics.

Published under an exclusive license by AIP Publishing. https://doi.org/10.1063/5.0071984

The ability of crafting materials at dimensions comparable to wavelengths of light not only allowed control of electromagnetic radiation at the nanoscale but also paved the way to revolutionary metamaterials[1] and photonic crystals (PCs).[2–4] PCs, periodically altering refractive index materials, reshape the propagation (dispersion) of the incident light and even can prevent it at certain propagation directions within some frequency ranges, named as photonic band gaps (PBGs).[5] PBGs, whose structure depends on the periodicity and index contrast, can be utilized as waveguides,[6] optical cavities,[7] optical memories,[8] and switches.[9,10] In this way, PBGs enable important applications such as on-chip photonic signal processing.[11] These structures allow control even over quantum phenomena[12–14] such as spontaneous emission[15,16] and entanglement[17] at the nanoscale.

Similar to resonator- and waveguide-based optical switches,[18–20] a PC based switch requires external control of the constituent material's refractive index. Tuning the PBG width a few percent allows for use of PCs as photonic switches. The refractive index of semiconductors (materials commonly employed in current PC technologies owing to their relatively high index, $n = 3.5$–4, and small absorption) can be tuned externally (actively) via optical heating,[21] free-carrier excitation,[18] and electronic Kerr-effect.[10,22] While the technique of free-carrier excitation provides the largest index change (∼3%), its response time (tens of picoseconds) is much longer compared to the modulation time of the Kerr effect (a few femtosecond). Using the Kerr effect, in contrast, an achievable index change is only ∼1%.

Metal nanostructures, which can localize the incident light into nm-sized hotspots, are also utilized for photonic technologies. Hybrid metastructures, created with semiconductors and metallic nanostructures, increase the versatility of integrated photonic structures.[23–25] Yet, the functionalities of modulation depth, response time, and (especially) metal-induced losses are limited.[23–25]

Therefore, a mechanism providing a large refractive index, which is tunable after the PC is manufactured with a short response time, would be very beneficial in the development of PC-based technologies. In this paper, we propose a control mechanism for PCs, which demonstrates all of the features listed above. We utilize a recently discovered extraordinary index enhancement (linear) scheme for coupled plasmonic nanorods.[26,27] A control pulse, of different polarizations, can tune the index up to an order of magnitude. The scheme is the analog of refractive index enhancement[28,29] previously used in creating the

Published under an exclusive license by AIP Publishing

PC from the vortex lattice of cold atoms,[30,31] a platform with limited technological potential.

In this paper, we show that the plasmon analog of index enhancement can carry PC-based technologies a step forward. The studied scheme can be used to create a stop band at a desired frequency, which is determined by the frequency and phase of the auxiliary (control) pulse. When the control pulse is off/on, the probe pulse is transmitted/reflected. Large modulation depths can be achieved even using 3–4 silver nanoparticle (NP) dimers. Once the structure is manufactured, the switch can be operated at different frequencies, which depends on the wavelength of the control pulse.

The operation principle of such a switch is quite different than the conventional ones. In the conventional PC switches, the device application is based on the 2%–3% tuning of the PBGs,[10,18,21,22] whereas, in our proposed method, the stop band appears at a specific frequency determined by the choice of the control pulse. Moreover, as the index enhancement is induced by the control pulse-driven nanorod, the response time is determined by the damping rates of the metal nanoparticles (MNPs), typically $\gamma_{MNP} = 10^{13}$–10^{15} Hz.[32,33]

Despite such rewards, it becomes necessary to tune the phase of the control pulse with respect to the lattice periodicity as the index is sensitive to the control pulse's phase. Such a tuning can be performed by using various alternative methods,[34–38] see the supplementary material for details. The stop band is achieved at the specific frequency determined by the control pulse, unlike conventional PC switches.[10,18,21,22] This provides flexibility in the operation frequency after manufacturing the miniature device.

We consider a 1D switch that contains 3–4 layers of nanorod dimers of total length 600–800 nm. We assume that the miniature switch is in a PC slab waveguide. Here, the PC waveguide is present only for confining and directing the light.[39] We perform 1D (modified) transfer matrix method (TMM) calculations for the 3–4 layer-length switch. We simulate each y-aligned nanorod as a uniform layer, whose effective index is tuned by the control pulse, see details in the text. In this initial work, we aim to present the idea and the basic behavior of such a switch without complicating the system. Our TMM simulations take the shifted phases at each layer into account, which sets the major sophistication here. The method is more general and can be applied also to 2D and 3D lattices by considering other resonating structures, see the text.

For creating a tunable stop band, we make use of the recently explored phenomenon: plasmon-analog of index enhancement.[26] While plasmon analogs of electromagnetically induced transparency (EIT),[28,40,41] in the linear (Fano resonances[42–44]) and nonlinear response,[45–48] have been demonstrated before, demonstration of the plasmon analog of index enhancement[49] could theoretically be obtained just recently.[26] The phenomenon is also demonstrated experimentally.[27]

Panahpour and colleagues[26] demonstrate that polarization response of a y-aligned silver nanorod to a y-polarized probe pulse can be controlled by the presence of an x-polarized control pulse, see Fig. 1. Owing to the shape resonance (selective coupling[50]) of nanorods, x,y-polarized pulses can excite "only" the x,y-aligned nanorods, respectively. Beyond studying the enhancement using a basic analytical model, which has widely been demonstrated to work very well for plasmonic path interference effects,[47,51,52] Panahpour and colleagues also demonstrated the phenomenon via numerical solutions of 3D

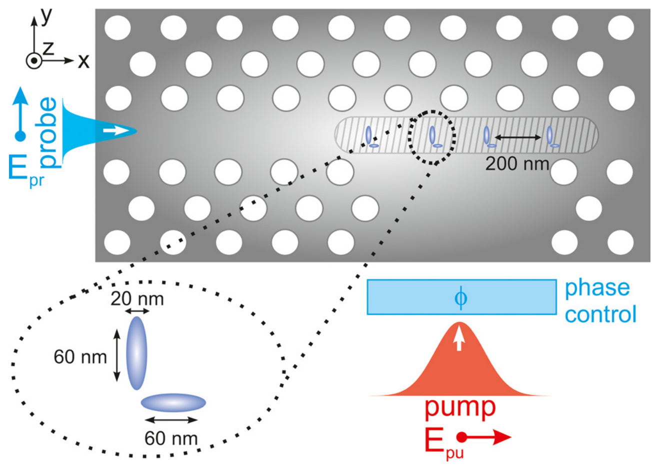

FIG. 1. A sample setup for the sub-micron photonic switch. The probe ($E_1\hat{y}$) and the control ($E_2\hat{x}$) pulses enter the 3–4 layers of nanorod dimers (see the inset) through defect waveguides. Amplitude and phase of the control pulse controls the index enhancement of the dimers. When the control pulse is off, the probe is transmitted, while transmission is avoided when the control pulse is on. The phase of the control pulse is tuned along the x-direction (see the text). 3–4 layers (= 600–800 nm) are enough to achieve high modulation depths, see Figs. 3 and 4.

Maxwell equations for silver nanorods of dimensions $20 \times 60 \times 20\,\text{nm}^3$. This scheme not only enhances the refractive index by an order of magnitude but also results in a canceled absorption at the enhancement frequency—just the same as in its EIT counterpart.[29]

For a monochromatic control pulse $\tilde{E}_2(t) = E_2 e^{-i\phi} e^{-i\omega t}$, of the same frequency with the probe $\tilde{E}_1(t) = E_1 e^{-i\omega t}$, the enhanced susceptibility seen by the probe (E_1) pulse can be expressed as[26,53]

$$\chi(\omega) = f\omega_0^2 \frac{\delta_2 + g e^{-i\phi} E_2/E_1}{\delta_1\delta_2 - g^2}, \tag{1}$$

where $\delta_i = \omega_i^2 - \omega^2 - i\gamma_i\omega$. $\omega_1 = \omega_2 = \omega_0$ and $\gamma_{1,2}$ are the resonances and the damping rates of the two nanorods, respectively. g defines the interaction strength between the two nanorods. $E_{1,2}$ are the amplitudes of the probe and control pulses, see the supplementary material for details. One can realize that the enhanced susceptibility $\chi(\omega)$ in Eq. (1) is strongly dependent on the phase difference ϕ between the probe and control pulses. For one choice of the ϕ, susceptibility can be enhanced (in a given frequency range) while such an enhancement may vanish for another choice of the ϕ.

Figure 2 plots the refractive index $n(\omega)$ for the probe pulse calculated from Eq. (1).[54] The index can be enhanced about three and six times for a control pulse of amplitudes $E_2 = 10E_1$ and $E_2 = 50E_1$, respectively. Moreover, the refractive index is real at $\omega = \omega_c = 0.965\omega_0$. Thus, one can tune the control pulse amplitude E_2 for altering the refractive index of the y-polarized probe pulse E_1 propagating in the x-direction. In Fig. 2(b), we observe that the imaginary part of the index becomes zero almost at the same frequency (vertical dashed-line) for $E_2 = 50E_1$ and $10E_1$, where the real part of the index becomes superiorly enhanced. We note that a double resonance appears for $E_2 = 0$ due to the presence of coupling between the two nanorods when the control pulse is turned off.

Published under an exclusive license by AIP Publishing

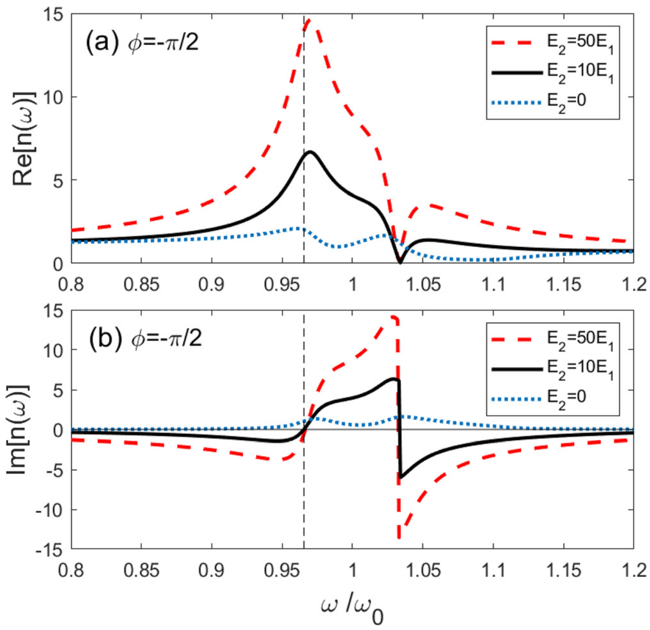

FIG. 2. (a) Real and (b) imaginary parts of the enhanced refractive index. Response (index) of the medium to the y-polarized probe pulse is controlled by the amplitude of the x-polarized control pulse (E_2). Index is enhanced, and it is real at $\omega_c = 0.965\omega_0$. Resonance of the nanorods is ω_0. Without the periodicity, the probe pulse is amplified, e.g., to the left of ω_c.

It is worth mentioning that the susceptibility (1), hence the refractive indices in Fig. 2, is sensitive to the phase difference ϕ. In Fig. 2, we consider a phase difference $\phi = -\pi/2$ between the probe and the control pulses. For other choices of ϕ, the index enhancement can appear at other frequencies or even disappear. Thus, phase tuning also provides another degree of freedom for achieving the desired function of the device.

We propose to utilize such nanorod dimers for manufacturing a miniaturized tunable photonic switch. We consider a system where 3–4 nanorod dimers are placed in a photonic crystal cavity depicted in Fig. 1. We take the periodicity of the dimers as a_x=200 nm in the x-direction. We consider the y, z dimensions of the cavity as $\ell_y = \ell_z = 100$ nm. Probe couples only to the y-aligned nanorod whose x-width is w_x=20 nm. We ignore interaction of the probe with the x-aligned nanorod, which is very small compared to its coupling to the y-aligned nanorod even without the index enhancement. That is, the layer in which only a single dimer exists has the volume $V_{layer} = 20 \times 100 \times 100\,\text{nm}^3$. V_{layer} has the index depicted in Fig. 2. We assume that the remaining part of the periodicity $V_{gap} = 180 \times 100 \times 100\,\text{nm}^3$ is filled with index $n = 1$. Filling factor of the index enhanced layer is 20/200 = 10%. The total length of the switch is 3–4 × 200 nm = 600–800 nm. The x-polarized control pulse propagates in the y-direction, and its phase can be altered along the x-direction. We carry out the reflection/transmission and propagation calculations using a transfer matrix method, which is adapted for the E_2/E_1-dependent (also phase-dependent) index calculated from $\chi(\omega)$ in Eq. (1), see the supplementary material for details. In all the calculations presented below, we set $E_2 = 10E_1$.

It is important to note that the index enhancement scheme presented in Fig. 2 is very sensitive to the phase difference ϕ between the probe and the control pulses. This means that, though we warranty the enhancement of the index at the first layer via an initial phase tuning, the susceptibility (1) may not be enhanced in the second or third layers. For circumventing this partially, we introduce an x-dependent phase to the control pulse. We set a $\phi_{ctrl}(x) = 2\pi[n(\omega) \times w_x + 1 \times (a_x - w_x)]/\lambda$ phase shift to the control pulse along the x-direction at each alternating layer. λ is the vacuum wavelength of the operation frequency. This can be performed, for instance, by using a spatial light modulator (SLM) in free space, a wedge geometry, or a photonic crystal waveguide design, see the supplementary material.

We note that this procedure only warranties the index enhancement at the second layer, e.g., not at the third layer. Worse, for any arrangement of the $\phi_{ctrl}(x)$ at the second layer, the E_2/E_1 ratio changes, which demolishes the periodicity of the index. Still, our calculations (Figs. 3 and 4) show that the method works for a wide range of frequencies, i.e., where an enhanced index is present. We kindly note the following. The frequency where the index becomes real, $\omega = 0.965\omega_0$, lies in the bandgap region, for instance, both for $E_2 = 10E_1$ and $E_2 = 50E_1$.

Figure 3 demonstrates the transmission after each layer when the control pulse is (a) off and (b) on. In Fig. 3(a), the transmitted pulse decreases linearly at a log plot. In Fig. 3(b), however, the slope of the transmission becomes steeper at each layer as E_2/E_1 changes at each layer. We observe in Fig. 4 that such a $\phi_{ctrl}(x)$ tuning works for a wide range of frequencies about the enhancement region. It is striking that: while there exists a large amount of gain at $\omega = 0.95\omega_0$ in Fig. 2(b), Fig. 4 shows that the stop band of the three-layer structure can turn-off the transmission.

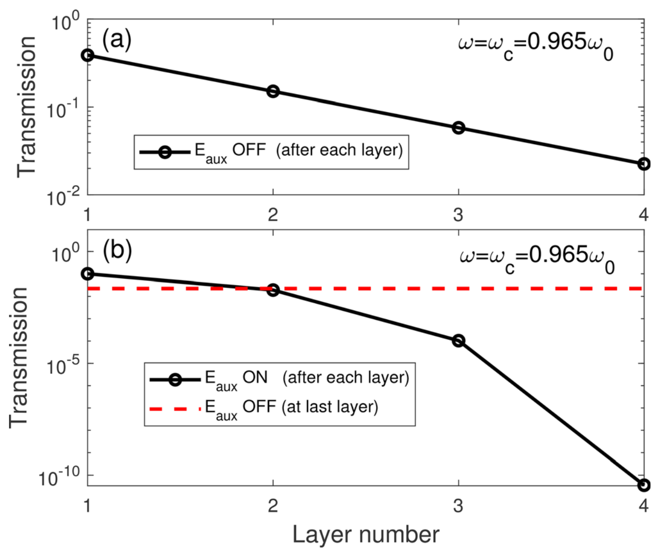

FIG. 3. Transmission of the probe after each layer. The control (auxiliary) pulse amplitude is set to $E_2 = 10E_1$ in all calculations. (a) When the control pulse is off, the index is not enhanced. The transmitted pulse is absorbed by the silver nanorods, and it decreases linearly in the semi-log scale. (b) When the control pulse is on, the index is enhanced (Fig. 2). The E_2/E_1 ratio changes at each layer, resulting in a larger susceptibility (1) at each alternating layer. The width of a layer, containing a single nanorod dimer, is 20 nm, and the periodicity is $a_x = 200$ nm.

Published under an exclusive license by AIP Publishing

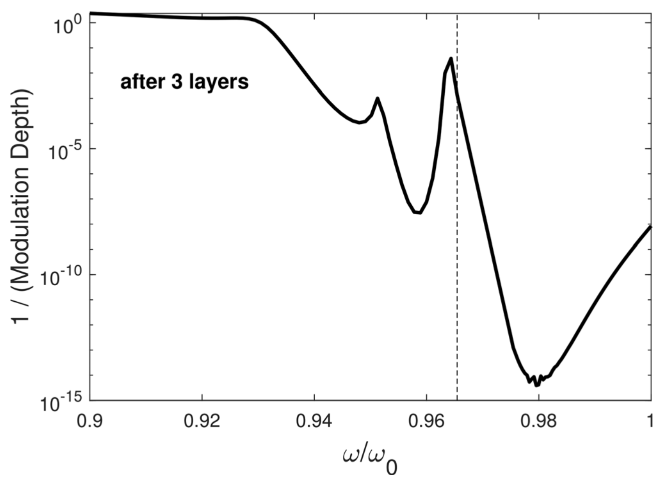

FIG. 4. Modulation depth achieved using only three layers of dimers of length = 3 × 200 nm = 600 nm. The modulation of the transmitted signal is compared with the $E_2 = 0$ (blue dashed-line in Fig. 2). Though there is gain for $\omega < \omega_c$=0.965ω_0, the index is enhanced, see black solid-line in Fig. 2; the three-layer structure stops the transmission with a modulation depth of 10^7 at about 0.96ω_0. Modulations depths as high as 10^{14} can be achieved.

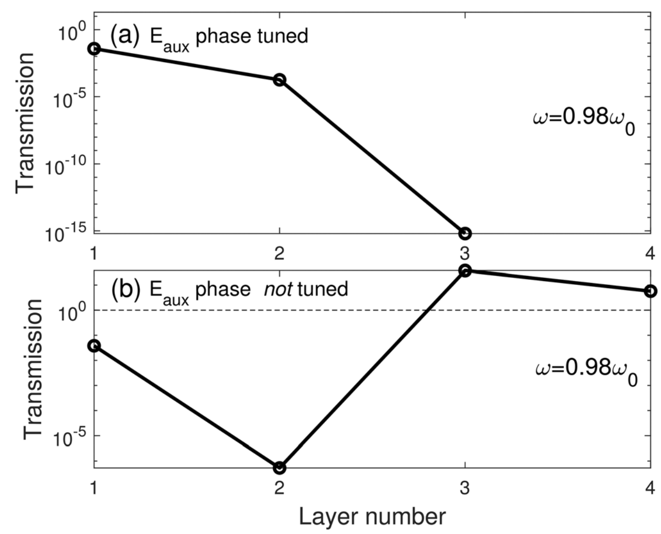

FIG. 5. A comparison of the behaviors of the transmission when the phase of the control pulse $\phi_{ctrl}(x)$ is (a) tuned and (b) not tuned. (a) When $\phi_{ctrl}(x)$ is tuned, each layer displays an enhanced index. (b) When the phase of the control pulse is not tuned, the first and the second layers suppress the transmission but the third layer amplifies the probe pulse. For a varied phase difference, e.g., for $\phi = +\pi/2$, the index displays a gain at the same frequency, see the supplementary material for the behavior of the refractive index for different phases.

In Fig. 5, we compare the two situations, i.e., when the phase tuning $\phi_{ctrl}(x)$ is (a) performed and (b) not performed at $\omega = 0.98\omega_0$. Figure 5(b) shows that the phase mismatch results a gain medium at the third layer. The behavior of the refractive index for other values of the phase difference can be found in the supplementary material One can observe that $n(\omega)$ displays a large gain at $\omega = 0.98\omega_0$, while there is a large absorptive imaginary part $\mathrm{Im}\{n(\omega)\}$ for $\phi = -\pi/2$ at $\omega = 0.98\omega_0$. In Fig. 5(a), we could not calculate the transmission after the fourth layer as the index $\sim(E_2/E_1)^{1/2}$ becomes extremely large and it appears in exponent in TMM calculations.

Figure 3(a) shows that even when the control intensity is off, i.e., the switch is ON, only 2% of the probe pulse is transmitted at $\omega = \omega_c = 0.965\omega_0$. While the transmission drops to 10^{-10} when the control pulse is on, this situation results in signal inefficiency in the switching operations. This problem can be circumvented by operating the switch by altering the phase of the control pulse $\phi_{crtl}(x)$. For instance, Fig. 5 compares the transmissions with and without an appropriate $\phi_{crtl}(x)$ phase tuning. One can observe [Fig. 5(b)] that after the third layer probe signal is even amplified by $\sim$20 times when the phase $\phi_{crtl}(x)$, while it is suppressed to 10^{-15} when the $\phi_{crtl}(x)$ phase is tuned accordingly.

The enhancement scheme possesses a remarkable advantage in photonic switch applications: the probe and the control pulses have different polarizations. Thus, Rayleigh scattering of the control pulse cannot limit the modulation depth. The modulation depth can be limited only by a polarization conversion scattering. Apart from the energy transfer at the hot spot, x and y-aligned nanorods possess very small polarization-converting scattering because of their shape resonances. The polarization conversion due to the energy transfer at the hot spot is already considered with the propagation of the probe pulse, and the phase is chosen accordingly. The main limiting factor for the modulation depth appears due to the radiative damping of the x-aligned nanorod along the x-direction. Yet, only 2% of the damping rate is due to the radiative decay in small nanoparticles,[55] and such limitations can also be circumvented by employing the switching via the phase-tuning method.

An index enhancement scheme depends critically on the phase difference between the probe and the control pulses. When there is periodicity of nanodimers along the z-axis in Fig. 1, there would appear no problems, because the phase of the control pulse is constant in the x-z plane. On working the periodicity along the propagation direction of the control pulse, y, however, one needs to take care of the different positions (so phases) of adjacent dimer arrays along the y-direction.

In summary, we demonstrate that a recently explored phenomenon, the plasmon analog of the index enhancement,[26] can be utilized for achieving a sub-micron-long photonic switch. Moreover, the operation frequency of the switch is tunable via a control pulse after it is manufactured. The method provides high modulation depths for a 3–4 layer structure, see Fig. 4. Such a micrometer-long switch is essential for the miniaturization of photonic devices and can be integrated into dielectric or nanoparticle waveguides.[56]

The index enhancement is obtained using two perpendicularly positioned silver nanorods of dimensions $20 \times 60 \times 60\,\mathrm{nm}^3$.[26] The response (index) of the system to the y-polarized probe pulse is tuned by an x-polarized auxiliary (control) pulse. The index becomes larger as the amplitude of the control pulse increases. Once the control pulse is turned off, the index enhancement would disappear in tens of femtoseconds, allowing the transmission of the probe pulse. The switch can also be operated by setting (OFF) and removing (ON) the appropriate phase-tuning for the control pulse. In the ON mode, the transmitted pulse is even amplified. The method is applicable also to 2D and 3D photonic structures.

Published under an exclusive license by AIP Publishing

Despite its advantages, the setup necessitates a careful tuning of the spatial phase $\phi_{ctrl}(x)$ of the control pulse along the periodicity (x) direction. This can be achieved either by tilting the propagation direction of the control pulse or by using a phase modulator.[37,38] While this may cause complications for longer switches, basic TMM simulations show that 3–4 layers should be enough for obtaining reliable modulation depths. In other words, we already aim to manufacture a short switch here.

In this work, we focus on a short switch application. However, the scheme and the method we introduce here can also be used to manufacture photonic waveguides, whose operation frequency can be tuned via a control pulse. This presents both size and control advantages compared to the conventional integrated photonic crystal waveguides, whose PBGs can only be tuned within a small range using the conventional tuning mechanisms. Moreover, the large modulation depth that we demonstrate here is of particular importance in achieving the integrated amplitude modulation. The conventional amplitude modulators that are based on nonlinear crystals are difficult to integrate on chip and require very large potentials that are not practical for integrated schemes. The method that we propose here is based on linear operation and has very small foot-print.

See the supplementary material for the details on the plasmon-analog of the index enhancement, the modified transfer matrix method, the methods for tuning the phase of the control pulse, the choice of the lattice parameter, and the maximum modulation depth.

M.E.T. acknowledges support from TUBA GEBIP 2017 and TUBITAK 1001, No. 117F118. R.S., A.B., and M.E.T. acknowledge support from TUBITAK 1001, No. 119F101. R.S. and M.E.T. acknowledge support from No. 121F030.

AUTHOR DECLARATIONS

Conflict of Interest

The authors have no conflicts to disclose.

DATA AVAILABILITY

The data that support the findings of this study are available from the corresponding author upon reasonable request.

REFERENCES

[1] Y. Liu and X. Zhang, "Metamaterials: A new frontier of science and technology," Chem. Soc. Rev. **40**, 2494–2507 (2011).
[2] E. Yablonovitch, "Inhibited spontaneous emission in solid-state physics and electronics," Phys. Rev. Lett. **58**, 2059 (1987).
[3] E. Yablonovitch, T. J. Gmitter, and K.-M. Leung, "Photonic band structure: The face-centered-cubic case employing nonspherical atoms," Phys. Rev. Lett. **67**, 2295 (1991).
[4] J. E. G. J. Wijnhoven and W. L. Vos, "Preparation of photonic crystals made of air spheres in titania," Science **281**, 802–804 (1998).
[5] M. D. Leistikow, A. P. Mosk, E. Yeganegi, S. R. Huisman, A. Lagendijk, and W. L. Vos, "Inhibited spontaneous emission of quantum dots observed in a 3D photonic band gap," Phys. Rev. Lett. **107**, 193903–1–5 (2011).
[6] J. C. Knight, T. A. Birks, P. S. J. Russell, and D. M. Atkin, "All-silica single-mode optical fiber with photonic crystal cladding," Opt. Lett. **21**, 1547–1549 (1996).
[7] Y. Akahane, T. Asano, B.-S. Song, and S. Noda, "High-Q photonic nanocavity in a two-dimensional photonic crystal," Nature **425**, 944–947 (2003).
[8] E. Kuramochi, K. Nozaki, A. Shinya, K. Takeda, T. Sato, S. Matsuo, H. Taniyama, H. Sumikura, and M. Notomi, "Large-scale integration of wavelength-addressable all-optical memories on a photonic crystal chip," Nat. Photonics **8**, 474–481 (2014).
[9] T. G. Euser, H. Wei, J. Kalkman, Y. Jun, A. Polman, D. J. Norris, and W. L. Vos, "Ultrafast optical switching of three-dimensional Si inverse opal photonic band gap crystals," J. Appl. Phys. **102**, 053111 (2007).
[10] E. Yüce, G. Ctistis, J. Claudon, E. Dupuy, R. D. Buijs, B. de Ronde, A. P. Mosk, J.-M. Gérard, and W. L. Vos, "All-optical switching of a microcavity repeated at terahertz rates," Opt. Lett. **38**, 374–376 (2013).
[11] J. Wang and Y. Long, "On-chip silicon photonic signaling and processing: A review," Sci. Bull. **63**, 1267–1310 (2018).
[12] S. Haroche and D. Kleppner, "Cavity quantum electrodynamics," Phys. Today **42**(1), 24–30 (1989).
[13] P. Lodahl, A. Floris Van Driel, I. S. Nikolaev, A. Irman, K. Overgaag, D. Vanmaekelbergh, and W. L. Vos, "Controlling the dynamics of spontaneous emission from quantum dots by photonic crystals," Nature **430**, 654–657 (2004).
[14] K. H. Madsen, S. Ates, T. Lund-Hansen, A. Löffler, S. Reitzenstein, A. Forchel, and P. Lodahl, "Observation of non-Markovian dynamics of a single quantum dot in a micropillar cavity," Phys. Rev. Lett. **106**, 233601 (2011).
[15] M. O. Scully, "Single photon subradiance: Quantum control of spontaneous emission and ultrafast readout," Phys. Rev. Lett. **115**, 243602 (2015).
[16] M. O. Scully and A. A. Svidzinsky, "The super of superradiance," Science. **325**, 1510–1511 (2009).
[17] M. E. Tasgin, "Many-particle entanglement criterion for superradiantlike states," Phys. Rev. Lett. **119**, 033601 (2017).
[18] V. R. Almeida, C. A. Barrios, R. R. Panepucci, and M. Lipson, "All-optical control of light on a silicon chip," Nature **431**, 1081–1084 (2004).
[19] Ö. Boyraz, P. Koonath, V. Raghunathan, and B. Jalali, "All optical switching and continuum generation in silicon waveguides," Opt. Express **12**, 4094–4102 (2004).
[20] O. Wada, "Femtosecond all-optical devices for ultrafast communication and signal processing," New J. Phys. **6**, 183 (2004).
[21] G. T. Reed and A. P. Knights, *Silicon Photonics: An Introduction* (John Wiley & Sons, 2004).
[22] G. Ctistis, E. Yuce, A. Hartsuiker, J. Claudon, M. Bazin, J.-M. Gérard, and W. L. Vos, "Ultimate fast optical switching of a planar microcavity in the telecom wavelength range," Appl. Phys. Lett. **98**, 161114 (2011).
[23] K. Fan and W. J. Padilla, "Dynamic electromagnetic metamaterials," Mater. Today **18**, 39–50 (2015).
[24] Q. He, S. Sun, L. Zhou *et al.*, "Tunable/reconfigurable metasurfaces: Physics and applications," Research **2019**, 1849272.
[25] L. Kang, R. P. Jenkins, and D. H. Werner, "Recent progress in active optical metasurfaces," Adv. Opt. Mater. **7**, 1801813 (2019).
[26] A. Panahpour, A. Mahmoodpoor, and A. V. Lavrinenko, "Refraction enhancement in plasmonics by coherent control of plasmon resonances," Phys. Rev. B **100**, 075427 (2019).
[27] R. Dhama, A. Panahpour, T. Pihlava, D. Ghindani and H. Caglayan, "All-optical switching via coherent control of plasmon resonances," Phys. Opt. arXiv:2111.07260v1.
[28] M. O. Scully and M. S. Zubairy, *Quantum Optics* (Cambridge University Press, New York, 1997).
[29] M. Fleischhauer, A. Imamoglu, and J. P. Marangos, "Electromagnetically induced transparency: Optics in coherent media," Rev. Mod. Phys. **77**, 633 (2005).
[30] M. E. Taşgın, Ö. E. Müstecaplıoğlu, and M. Ö. Oktel, "Photonic band gap in the triangular lattice of Bose-Einstein-condensate vortices," Phys. Rev. A **75**, 063627 (2007).
[31] Ö. E. Müstecapl ioğlu and M. Ö. Oktel, "Photonic band gap via quantum coherence in vortex lattices of Bose-Einstein condensates," Phys. Rev. Lett. **94**, 220404 (2005).
[32] I. Zoric, M. Zach, B. Kasemo, and C. Langhammer, "Gold, platinum, and aluminum nanodisk plasmons: Material independence, subradiance, and damping mechanisms," ACS Nano **5**, 2535–2546 (2011).
[33] B. C. Yildiz, A. Bek, and M. E. Tasgin, "Plasmon lifetime enhancement in a bright-dark mode coupled system," Phys. Rev. B **101**, 035416 (2020).

Published under an exclusive license by AIP Publishing

[34]E. Yuce, J. Lian, S. Sokolov, J. Bertolotti, S. Combrie, G. Lehoucq, A. De Rossi, and A. P. Mosk, "Adaptive control of necklace states in a photonic crystal waveguide," ACS Photonics **5**, 3984–3988 (2018).
[35]J. Schrauwen, S. Scheerlinck, D. Van Thourhout, and R. Baets, "Polymer wedge for perfectly vertical light coupling to silicon," Proc. SPIE **7218**, 72180B (2009).
[36]Y. Zhang and B. Li, "Photonic crystal-based bending waveguides for optical interconnections," Opt. Express **14**, 5723–5732 (2006).
[37]C. Kohler, F. Zhang, and W. Osten, "Characterization of a spatial light modulator and its application in phase retrieval," Appl. Opt. **48**, 4003–4008 (2009).
[38]R. Amin, R. Maiti, J. B. Khurgin, and V. J. Sorger, "Performance analysis of integrated electro-optic phase modulators based on emerging materials," IEEE J. Sel. Top. Quantum Electron. **27**(3), 3300211 (2021).
[39]In case of an unconfined light, one can also alternate the 3–4 layer structure along the y-direction.
[40]M. D. Lukin and A. Imamoğlu, "Controlling photons using electromagnetically induced transparency," Nature **413**, 273–276 (2001).
[41]K.-J. Boller, A. Imamoğlu, and S. E. Harris, "Observation of electromagnetically induced transparency," Phys. Rev. Lett. **66**, 2593 (1991).
[42]B. Luk'yanchuk, N. I. Zheludev, S. A. Maier, N. J. Halas, P. Nordlander, H. Giessen, and C. T. Chong, "The fano resonance in plasmonic nanostructures and metamaterials," Nat. Mater. **9**, 707 (2010).
[43]M. F. Limonov, M. V. Rybin, A. N. Poddubny, and Y. S. Kivshar, "Fano resonances in photonics," Nat. Photonics **11**, 543 (2017).
[44]B. Peng, Ş. Kaya Özdemir, W. Chen, F. Nori, and L. Yang, "What is and what is not electromagnetically induced transparency in whispering-gallery microcavities," Nat. Commun. **5**, 5082 (2014).
[45]J. Butet and O. J. Martin, "Fano resonances in the nonlinear optical response of coupled plasmonic nanostructures," Opt. Express **22**, 29693–29707 (2014).
[46]S. K. Singh, M. K. Abak, and M. E. Tasgin, "Enhancement of four-wave mixing via interference of multiple plasmonic conversion paths," Phys. Rev. B **93**, 035410 (2016).
[47]M. E. Taşgin, A. Bek, and S. Postac i, "Fano resonances in the linear and nonlinear plasmonic response," in *Fano Resonances in Optics and Microwaves* (Springer, 2018), pp. 1–31.
[48]S. Postaci, B. C. Yildiz, A. Bek, and M. E. Tasgin, "Silent enhancement of SERS signal without increasing hot spot intensities," Nanophotonics **7**, 1687–1695 (2018).
[49]M. O. Scully, "Enhancement of the index of refraction via quantum coherence," Phys. Rev. Lett. **67**, 1855 (1991).
[50]D. Andrews, T. Nann, and R. H. Lipson, *Comprehensive Nanoscience and Nanotechnology* (Academic Press, 2019).
[51]X. Wu, S. K. Gray, and M. Pelton, "Quantum-dot-induced transparency in a nanoscale plasmonic resonator," Opt. Express **18**, 23633–23645 (2010).
[52]A. Lovera, B. Gallinet, P. Nordlander, and O. J. Martin, "Mechanisms of Fano resonances in coupled plasmonic systems," ACS Nano **7**, 4527–4536 (2013).
[53]M. Günay, Y.-L. Chuang, and M. E. Tasgin, "Continuously-tunable Cherenkov-radiation-based detectors via plasmon index control," Nanophotonics **9**, 1479–1489 (2020).
[54]M. Fleischhauer, C. H. Keitel, M. O. Scully, C. Su, B. T. Ulrich, and S.-Y. Zhu, "Resonantly enhanced refractive index without absorption via atomic coherence," Phys. Rev. A **46**, 1468 (1992).
[55]C. Sönnichsen, T. Franzl, T. Wilk, G. v. Plessen, J. Feldmann, O. V. Wilson, and P. Mulvaney, "Drastic reduction of plasmon damping in gold nanorods," Phys. Rev. Lett. **88**, 077402 (2002).
[56]S. A. Maier, P. G. Kik, and H. A. Atwater, "Optical pulse propagation in metal nanoparticle chain waveguides," Phys. Rev. B **67**, 205402 (2003).

Published under an exclusive license by AIP Publishing